

PCT



Report No. 92

UNITED STATES  
DEPARTMENT OF THE INTERIOR  
BUREAU OF MINES  
HELIUM ACTIVITY  
HELIUM RESEARCH CENTER  
  
INTERNAL REPORT

CONCERNING PHYSICAL PARAMETERS

FOR USE IN AN ABSOLUTE GAS VISCOSIMETER

BY

R. A. Guereca

H. P. Richardson

J. L. Gordon

J. E. Miller

BRANCH BRANCH OF FUNDAMENTAL RESEARCH

PROJECT NO. 5574

DATE July 1966

HD  
9660  
.H43  
M56  
no. 92

AMARILLO, TEXAS







#929458534

ID 88070882

FD  
9660  
.H43  
M56  
no.92

Report No. 92

CONTENTS

HELIUM RESEARCH CENTER

INTERNAL REPORT

CONCERNING PHYSICAL PARAMETERS  
FOR USE IN AN ABSOLUTE GAS VISCOSIMETER

By

R. A. Guereca, H. P. Richardson,  
J. L. Gordon, and J. E. Miller

BRANCH OF FUNDAMENTAL RESEARCH

Project 5574

July 1966

BLM Library  
Denver Federal Center  
Bldg. 50, OC-521  
P.O. Box 25047  
Denver, CO 80225

HEALTH RESEARCH CENTER

INTERNAL REPORT

DETERMINING PHYSICAL PARAMETERS  
FOR USE IN AN ABSOLUTE CAP VISCOSIMETER

2

J. A. Gordon, R. P. Richardson,  
J. M. Gordon, and J. E. Hunter

BRANCH OF FUNDAMENTAL RESEARCH

Project 2374

July 1966

Health Research  
Center, Federal Center  
Bldg. 30, Rm. 321  
PO Box 25047  
Denver, CO 80225



## CONTENTS

	<u>Page</u>
Abstract . . . . .	4
Introduction . . . . .	4
Measurement program . . . . .	7
Measurements and equipment precision and accuracy capability . . . . .	9
Confirmation of mean radius through Talyron charts . . . . .	19
Correction for non-uniformity of capillary bore . . . . .	23
Pressure and temperature level effects on mean radius and capillary length . . . . .	25
Average radius and density evaluation by different methods . . . . .	27
Entrance, kinetic energy, gas slippage, and gas compressibility effects . . . . .	28
Entrance and kinetic energy effects . . . . .	30
Gas slippage and gas compressibility effects . . . . .	31
Summary . . . . .	33
References . . . . .	35



CONTENTS

Page	
4	Abstract
5	Introduction
7	Measurement program
8	Measurements and equipment precision and accuracy capability
12	Confirmation of mean radius through Taylor's charts
23	Correction for non-uniformity of capillary bore
25	Pressure and temperature level effects on mean radius and capillary length
27	Average radius and density evaluation by different methods
28	Entrance, kinetic energy, gas slippage, and gas compressibility effects
30	Entrance and kinetic energy effects
31	Gas slippage and gas compressibility effects
32	Summary
33	References



## ILLUSTRATIONS

<u>Fig.</u>	<u>Page</u>
1. Fixture for length of bore measurements . . . . .	8
2. Fixture for ID measurements and out-of-roundness profiles . . . . .	8
3. Longitudinal view of capillary internal surface . . . . .	9
4. End view of capillary bores . . . . .	9
5. Cross section profile of a circular capillary bore . . . . .	10
6. Cross section profile of a trilobular capillary bore . . . . .	15
7. Cross section profile of an irregular capillary bore . . . . .	15
8. Deviation of the capillary bore from the average radius . . . . .	24
9. Distribution of SIP diameter measurements . . . . .	24

## TABLES

1. Internal diameter measurements . . . . .	11
2. External diameter measurements . . . . .	16
3. Length and mass measurements . . . . .	18
4. Radii computed by integrating the Talyrond charts. . . . .	21
5. Average radius and density evaluation by different methods . . . . .	29



ILLUSTRATIONS

<u>Page</u>	<u>Fig.</u>
8	1. Picture for length of bore measurements
8	2. Picture for ID measurements and out-of-roundness profiles
9	3. Longitudinal view of capillary internal surface
9	4. End view of capillary bore
10	5. Cross section profile of a circular capillary bore
12	6. Cross section profile of a lobular capillary bore
12	7. Cross section profile of an irregular capillary bore
14	8. Deviation of the capillary bore from the average radius
14	9. Distribution of 319 diameter measurements

TABLES

11	1. Internal diameter measurements
10	2. External diameter measurements
18	3. Length and mass measurements
21	4. Radii computed by integrating the Taylor chart
23	5. Average radius and density evaluation by different methods



CONCERNING PHYSICAL PARAMETERS  
FOR USE IN AN ABSOLUTE GAS VISCOSIMETER

by

R. A. Guereca,<sup>1/</sup> H. P. Richardson,<sup>2/</sup>  
J. L. Gordon,<sup>2/</sup> and J. E. Miller<sup>2/</sup>

ABSTRACT

Accurate measurements of physical dimensions of a section of stainless steel capillary tubing are presented and used to develop a final working equation for an absolute gas viscosimeter. The effects of pressure and temperature on these dimensions are considered. The internal surface finish and non-uniformity of the capillary bore are discussed as well as entrance, kinetic energy, gas slippage, and gas compressibility correction factors.

INTRODUCTION

The Bureau of Mines Helium Research Center is using a 208-foot long, thick-walled, stainless steel capillary tube, 0.030 inch in internal diameter, wound in the form of a helix 20 inches in diameter,

---

<sup>1/</sup>Supervisory Research Chemist, Project Leader, Physical Properties Studies, Helium Research Center, Bureau of Mines, Amarillo, Texas.  
<sup>2/</sup>Research Chemist, Helium Research Center, Bureau of Mines, Amarillo, Texas.



CONVERTING PHYSICAL PARAMETERS  
FOR USE IN AN ABSOLUTE GAS VISCOSIMETER

BY

R. A. Gault, R. E. Richardson,  
J. L. Gordon, and J. E. Miller

ABSTRACT

Accurate measurements of physical dimensions of a section of stainless steel capillary tubing are presented and used to develop a final working equation for an absolute gas viscosimeter. The effects of pressure and temperature on these dimensions are considered. The internal surface finish and non-uniformity of the capillary bore are discussed as well as entrance, kinetic energy, gas slipage, and gas compressibility correction factors.

INTRODUCTION

The Bureau of Mines Helium Research Center is using a 308-foot long, thick-walled, stainless steel capillary tube, 0.030 inch in internal diameter, wound in the form of a helix 30 inches in diameter.

Supervisor Research Chemist, Project Leader, Physical Properties  
Studies, Helium Research Center, Bureau of Mines, Aerial, Texas  
Research Chemist, Helium Research Center, Bureau of Mines, Aerial,  
Texas

Work on manuscript completed July 1955.



to determine viscosities for pure gases and mixtures at high pressure levels. A coiled capillary of the above dimensions is necessary at high pressures in order to obtain accurately measurable pressure drops at very low volumetric flowrates and to maintain a uniform temperature over the entire length; further, certain correction factors are minimized. Absolute viscosities, reproducible to an accuracy of one micropoise or better, are being evaluated. The values are absolute, insofar as calibration with a gas of known viscosity is not required. Prior to this, a 32-foot long capillary of the same dimensions was used for the experimental determination of steady-state laminar flow boundary conditions applicable to the coiled system.

Accurate measurements of the physical dimensions of a capillary section were made by the Atomic Energy Commission Pantex Plant, Amarillo, Texas. All measurements were taken under controlled environmental conditions.

The intent of this report is to present these measurements, show how they are used in determining certain physical parameters of interest, and develop a viscosity equation which includes corrections for the effects of the temperature and pressure levels on these parameters. The parameters are: mean radius,  $R_m$ , of the capillary tubing; variation of individual radii,  $R_i$ , with length,  $L_i$ ; and total length,  $L_T$ .

The correction for non-uniformity of the capillary bore or variations in  $R_i$  along  $L_T$  is shown to be negligible through the use of a correction factor,  $\delta$ . In a later section, the entrance or Couette cor-



to determine viscosities for pure gases and mixtures at high pressures  
levels. A coiled capillary of the above dimensions is necessary at  
high pressures in order to obtain accurately measurable pressure drops  
at very low volumetric flow rates and to maintain a uniform temperature  
over the entire length; further, certain correction factors are mini-  
mized. Absolute viscosities, reproducible to an accuracy of one  
microcent or better, are being evaluated. The values are absolute,  
insofar as calibration with a gas of known viscosity is not required.  
Prior to this, a 21-foot long capillary of the same dimensions was used  
for the experimental determination of steady-state laminar flow boundary  
conditions applicable to the coiled system.

Accuracy measurements of the physical dimensions of a capillary  
section were made by the Atomic Energy Commission Radioisotope Division,  
Texas. All measurements were taken under controlled environmental con-  
ditions.

The intent of this report is to present these measurements, show  
how they are used in determining certain physical parameters of interest,  
and develop a viscosity equation which includes corrections for the  
effects of the temperature and pressure levels on these parameters. The  
parameters are: mean radius,  $R_w$ , of the capillary tubing; variation of  
individual radii,  $R_i$ , with length,  $L_i$ ; and total length,  $L_T$ .

The correction for non-uniformity of the capillary bore or varia-  
tion in  $R_i$  along  $L_i$  is shown to be negligible through the use of a  
correction factor,  $K$ . In a later section, the entrance or Couette cor-



rection, involving  $R_m$  and  $L_T$ , is shown to be negligible; the kinetic energy correction, involving  $R_m^4$  when expressed in pressure units, and gas slippage at the walls of the capillary, involving  $R_m$  and the mean free path of the molecules,  $\lambda$ , also are shown to be negligible at the pressure and temperature levels of interest. The effect of gas compressibility, which does not involve a direct metrological determination, is discussed and shown to be negligible because of the very low pressure drops in the system.

At a given temperature (T) and pressure (P), the modified Poiseuille equation, incorporating the physical parameters just mentioned, is:

$$\eta = \left[ \frac{\pi R_m^4 \Delta P_e}{8L_T \delta Q_m} \right]_{(T,P)}, \quad (1)$$

where

- $\eta$  = computed viscosity at (T,P), poises;
- $R_m$  = mean radius of the capillary tube if the bore were uniform throughout, cm;
- $\Delta P_e$  = effective pressure drop used to overcome viscous resistance; measured pressure drop ( $\Delta P_{me}$ ) corrected for kinetic energy effects, dynes/cm<sup>2</sup>;
- $L_T$  = total length of capillary, cm;
- $\delta$  = correction of actual capillary bore from a uniform, right circular cylinder, dimensionless;
- $Q_m$  = mean volumetric gas flow rate, cm<sup>3</sup>/sec, at the mean system pressure,  $P_m$ .



reaction, involving  $R_0$  and  $R_1$ , is shown to be negligible; the kinetic energy correction, involving  $R_0^4$  when expressed in pressure units, and gas leakage at the walls of the capillary, involving  $R_0$  and the mean free path of the molecules,  $\lambda$ , also are shown to be negligible at the pressure and temperature levels of interest. The effect of gas compressibility, which does not involve a direct mechanical balance relation, is discussed and shown to be negligible because of the very low pressure drops in the system.

At a given temperature ( $T$ ) and pressure ( $P$ ), the modified Poiseuille equation, incorporating the physical parameters just mentioned,

$$(1) \quad \left[ \frac{\pi R_0^4 \Delta P}{8 \eta L T} \right]_{(T,P)} = \dot{V}$$

- where
- $\dot{V}$  = computed viscosity at ( $T, P$ ), poise;
  - $R_0$  = mean radius of the capillary tube if the ends were uniform throughout, cm;
  - $\Delta P_0$  = effective pressure drop used to overcome viscous resistance; measured pressure drop ( $\Delta P_m$ ) corrected for kinetic energy effects,  $\text{dynes/cm}^2$ ;
  - $L$  = total length of capillary, cm;
  - $\lambda$  = correction of actual capillary bore from a uniform, right circular cylinder, dimensionless;
  - $R_0$  = mean volumetric gas flow rate,  $\text{cm}^3/\text{sec}$ , at the mean system pressure,  $P$ .



A vertical volumetric rate pump circulates gas isothermally through the capillary at a constant mean rate,  $Q_m$ ; the pressure drop is measured by a precision-delta-pressure transducer. It is tacitly assumed that any basic errors in  $Q_m$  and  $\Delta P_{me}$  are negligible. Once the physical parameters  $R_m$ ,  $L_T$ , and  $\delta$  are known, as well as the effects of temperature and pressure on  $R_m$  and  $L_T$ , the determination of viscosity basically involves plotting a series of values of  $\Delta P_e$  versus  $Q_m$  on rectangular coordinates and determining the slope of this straight line.

The necessity for highly accurate and precise physical measurements can be noted from equation (1) where  $R_m$  is raised to the fourth power. Assuming all other terms to be correct, if  $R_m$  is known to within  $5 \times 10^{-6}$  inch, the computed viscosity will be within 0.25 micropoise when the true value is of the order of 200 micropoises.

#### MEASUREMENT PROGRAM

The original measurement program was designed to cross-check  $R_m$  by two methods. The "metrometric" method consisted of measurements of out-of-roundness, internal diameters (ID), and internal roughness of 4-inch sections of the capillary. The "volumetric" method included measurements of the length, external diameters (OD), and weights of 12-inch sections. If the density is accurately known and is uniform, the volumetric method can be used to compute the ID of the capillary bore. All measurements were made at  $293^\circ$  K and 0 psig.

Measurements were taken on a 19-foot section selected at random from 1,000 feet of 347 stainless steel tubing supplied by Superior Tube



A vertical volumetric rate tube circulates gas isothermally through the capillary at a constant mean rate,  $Q_m$ ; the pressure drop is measured by a precision-delta-pressure transducer. It is easily assumed that any basic errors in  $Q_m$  and  $\Delta P_m$  are negligible. Once the physical parameters  $R$ ,  $L$ ,  $\mu$ , and  $\delta$  are known, as well as the effects of temperature and pressure on  $R$  and  $L$ , the determination of viscosity basically involves plotting a series of values of  $\delta$  versus  $Q_m$  on rectangular coordinates and determining the slope of this straight line. The necessity for highly accurate and precise physical measurements can be noted from equation (1) where  $\delta$  is related to the fourth power. Assuming all other terms to be constant, if  $R$  is known to within  $2 \times 10^{-3}$  inch, the computed viscosity will be within 0.2% irrespective of the true value is of the order of 100 micropoise.

#### MEASUREMENT PROGRAM

The original measurement program was designed to cross-check  $R$  by two methods. The "volumetric" method consisted of measurements of one-of-roughness, internal diameter (ID), and internal roughness of 4-inch sections of the capillary. The "volumetric" method included measurements of the length, external diameter (OD), and weight of 12-inch sections. If the density is accurately known and is uniform, the volumetric method can be used to compute the ID of the capillary pore. All measurements were made at 293° K and 0 psig. Measurements were taken on a 19-foot section selected at random from 1,000 feet of 347 stainless steel tubing supplied by Superior Tube



Company.<sup>3/</sup> This "precision drawn instrument tubing" is nominally 0.122-

---

<sup>3/</sup>Trade names are used for information only and endorsement by the Bureau of Mines is not implied.

---

inch OD and 0.030-inch ID. Average mechanical properties are: 149,500-psig ultimate tensile strength and 136,400-psig yield strength.

The 19-foot section was cut into 1-foot lengths for the volumetric program. Each segment was formed into a circular arc with a 10.00000-inch radius of curvature, using a special fixture (figure 1) because

---

Figure 1.-Fixture for length of bore measurements.

---

the viscosimeter tubing is wound into a 20-inch diameter helix. The length and four OD's were measured for each section. The 1-foot lengths were weighed on an analytical balance before being cut into three 4-inch lengths. At each end of the 4-inch samples, three ID's, 60 degrees apart, were measured at a depth of 1/16 inch, and a profile of the out-of-roundness was taken at the same depth. The 4-inch samples were held in another fixture (figure 2) constructed to have the same 10.00000-inch

---

Figure 2.-Fixture for ID measurements and out-of-roundness profiles.

---

radius of curvature. By the above procedure, a total of 114 out-of-







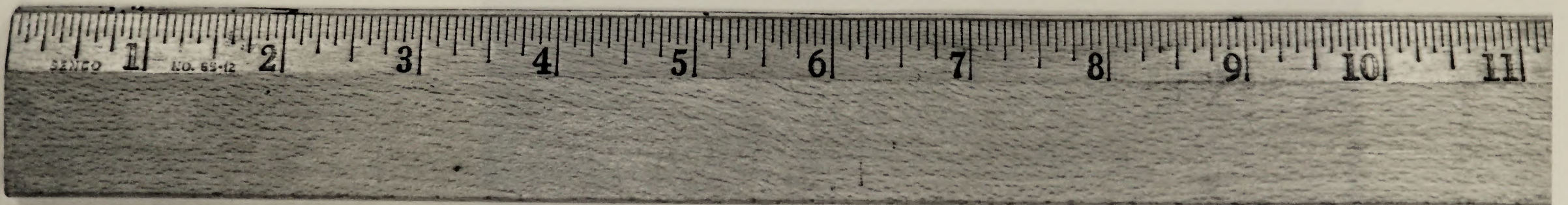
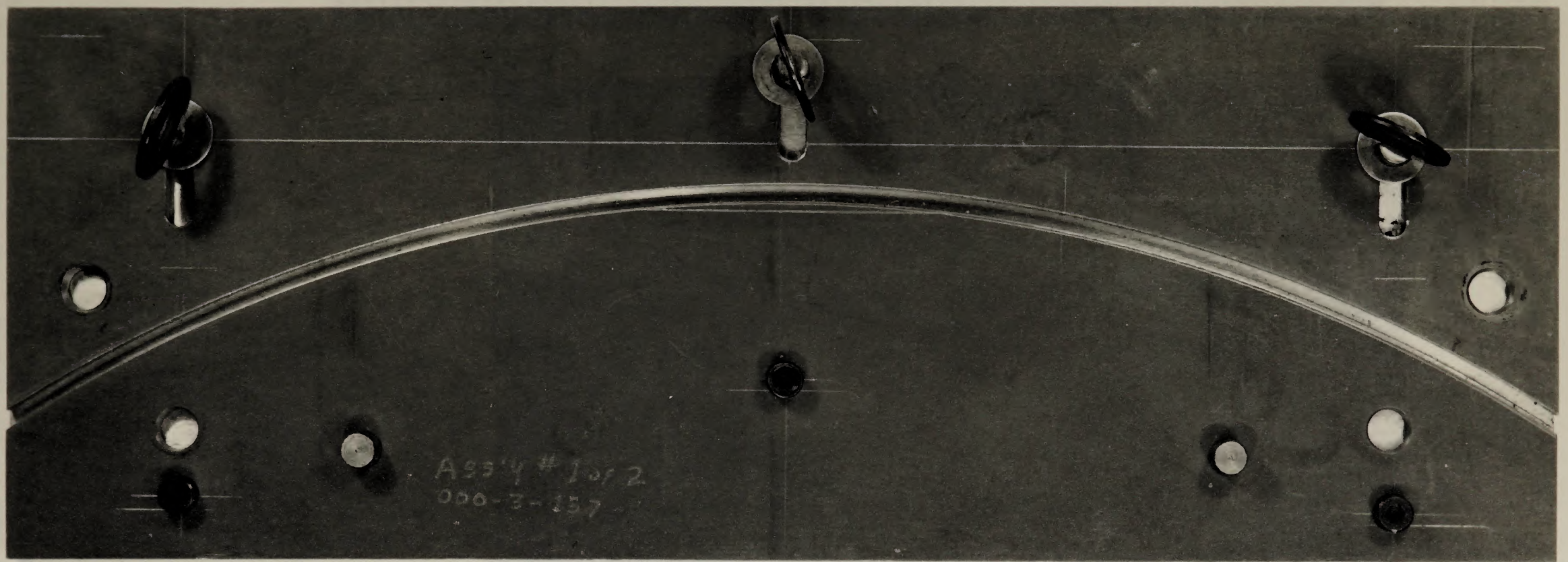


FIGURE 1.— Fixture for Length of Bore Measurements



Handwritten text, possibly bleed-through from the reverse side of the page.



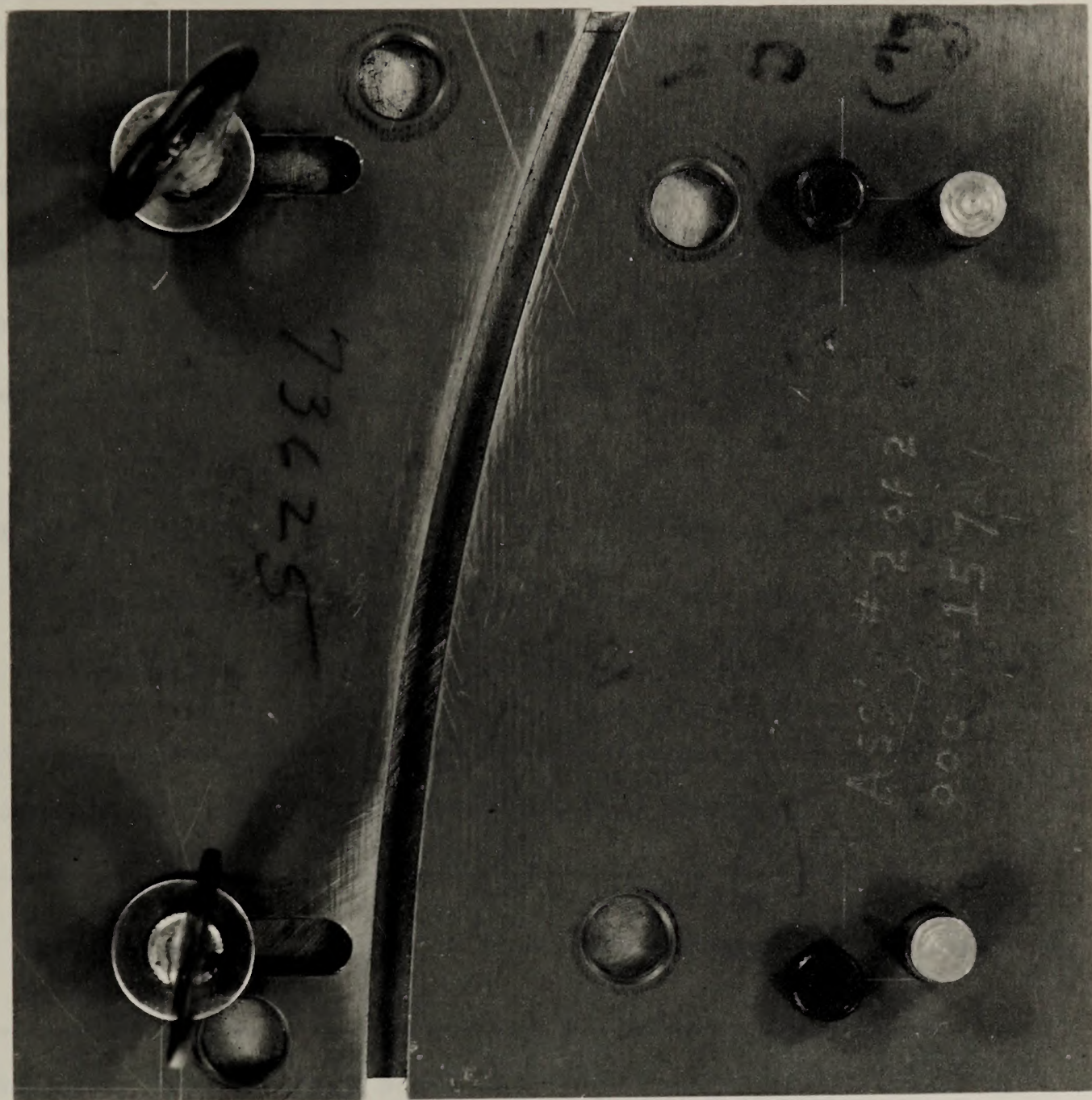
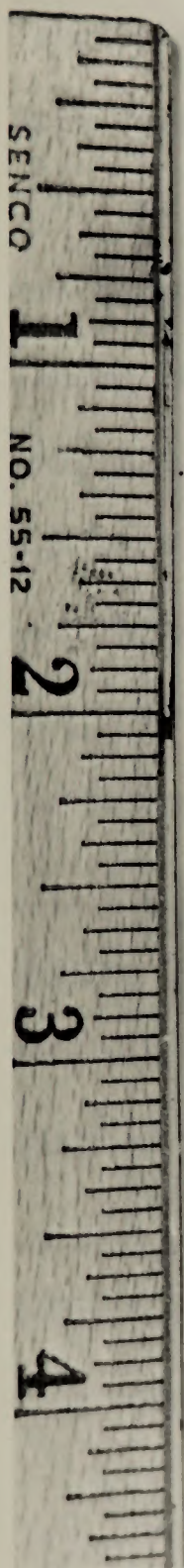


FIGURE 2.—Fixture for ID Measurements and Out-of-Roundness Profiles



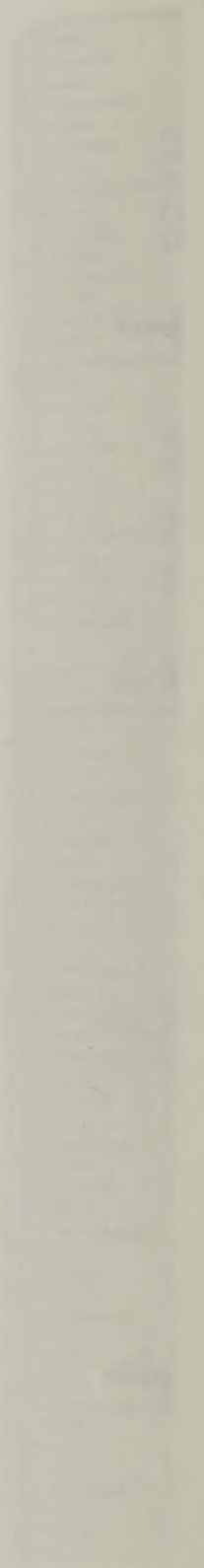


FIGURE 2-Frame for ID Measurements and  
Out-of-Balance Profile



roundness profiles and 342 ID measurements was made. Six of the 4-inch lengths were randomly selected for longitudinal internal finish or surface roughness measurements.

The desired lengths were cut with a saw and the ends ground smooth and square with a surface grinder to minimize distortion and provide a smooth reference surface. The surface grinder also was used to expose the inner surface for internal roughness determinations. A microscope was used to examine exposed internal surfaces. No evidence of distortion was found at the measurement depth. The out-of-roundness apparatus also was used to examine cross section profiles at various depths and showed no evidence of distortion due to cutting. Figure 3 shows a longitudinal

---

Figure 3.-Longitudinal view of capillary internal surface.

---

view of the internal surface; figure 4 shows end views of the capillaries.

---

Figure 4.-End view of capillary bores.

---

#### MEASUREMENTS AND EQUIPMENT PRECISION AND ACCURACY CAPABILITY

The ID's were measured with a Societe Genevoise D'Instruments De Physique Universal Measuring Machine, Model MU-214B, called the "SIP." A special gaging stylus, 0.005 inch in radius, was fabricated and used in conjunction with the holding fixture which vertically supported the capillary sections. Individual diameters measured with this instrument







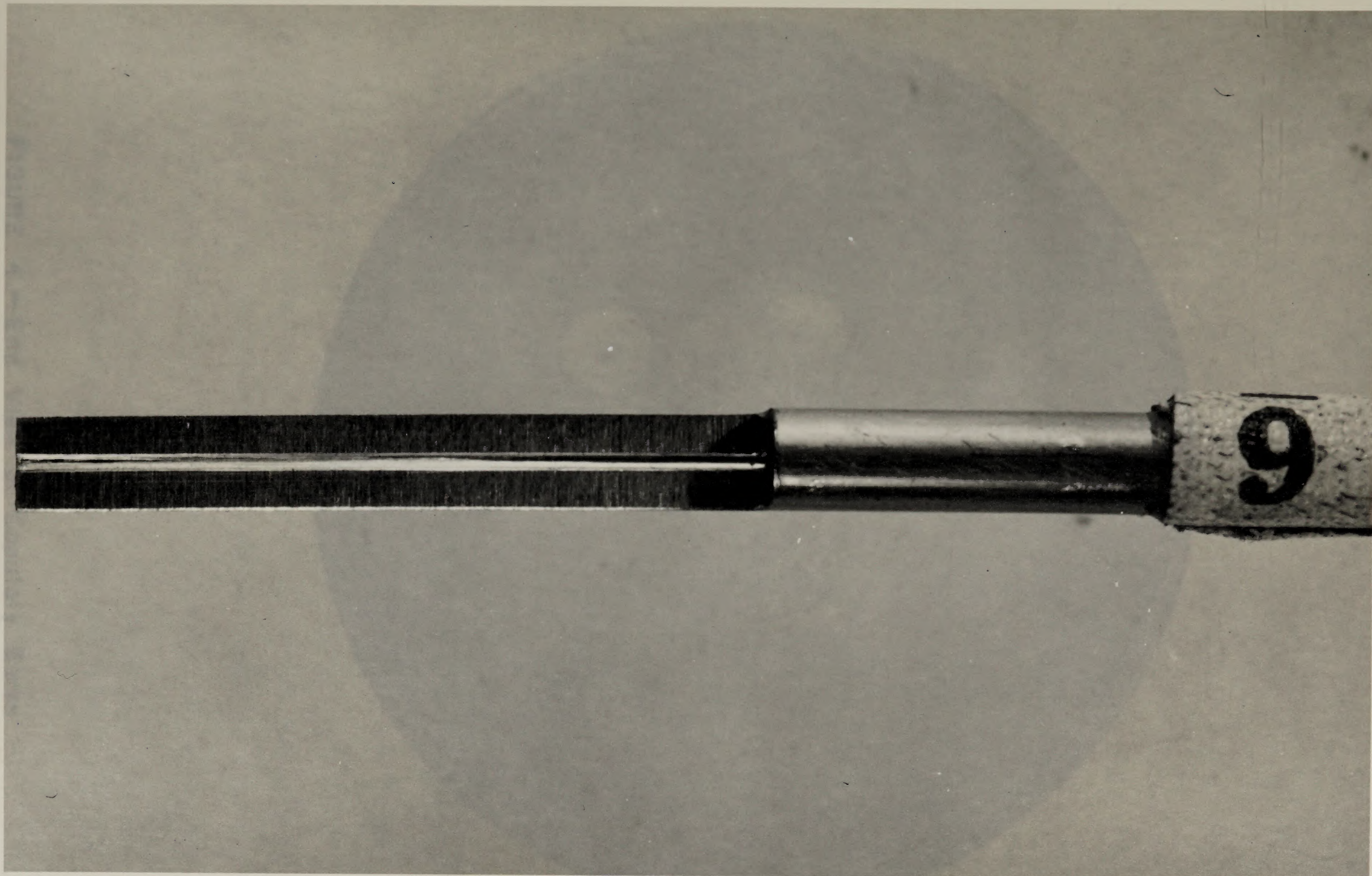


FIGURE 3.— Longitudinal View of Capillary Internal Surface



КОНЦЕ 2 - Гробишта на манастирскиот комплекс

9



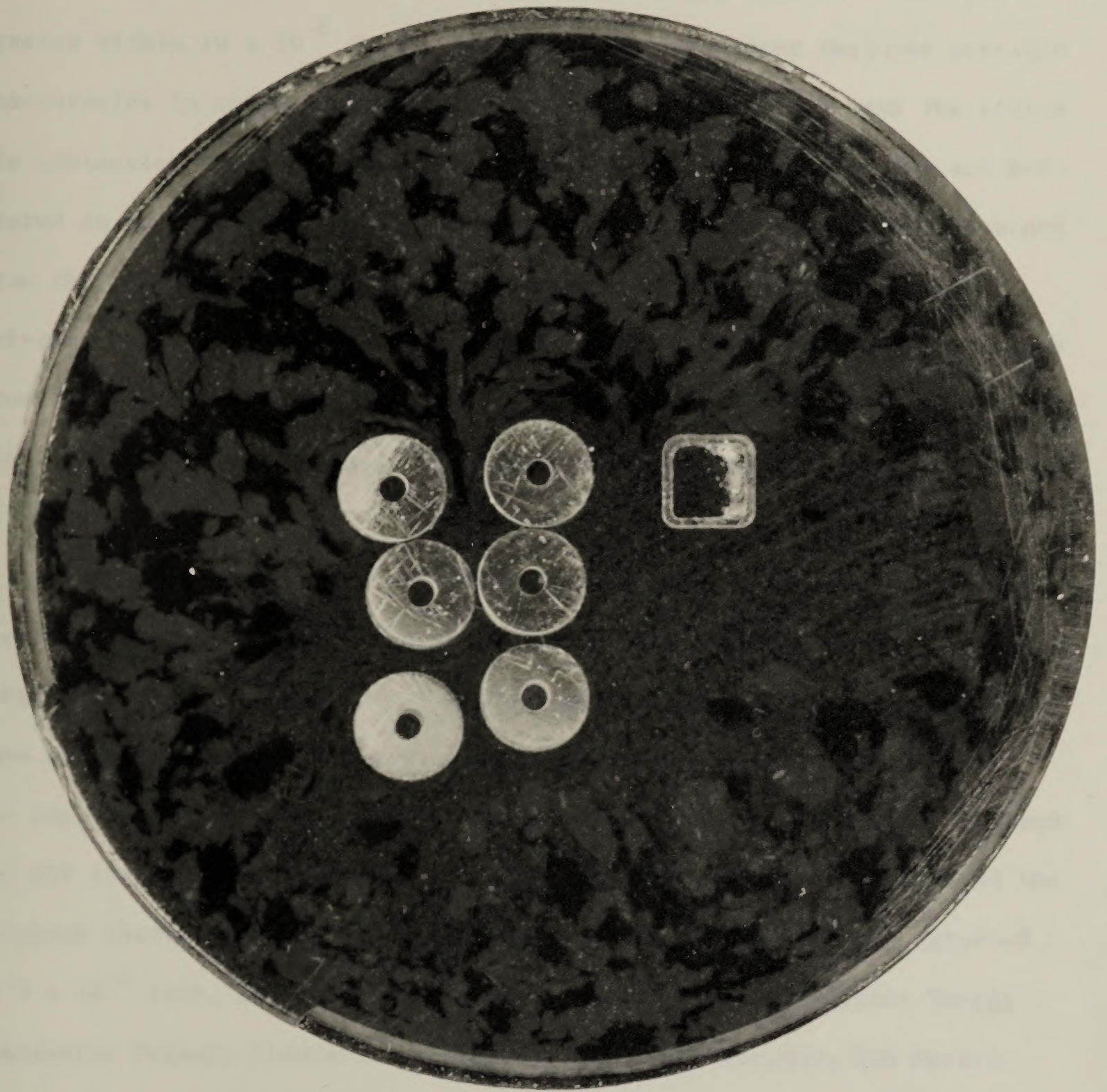


FIGURE 4.—End View of Capillary Bores







were conservatively estimated to be accurate within  $20 \times 10^{-6}$  inch and precise within  $10 \times 10^{-6}$  inch. The error of measurement includes possible inaccuracies in stylus deflection, internal surface finish, and the stylus tip contacting the inner surface. Results of the ID measurements are presented in table 1 and include the average radius for each section obtained from the  $0^\circ$ ,  $60^\circ$ , and  $120^\circ$  SIP measurements; each 4-inch length had a reference mark on both ends to represent the  $0^\circ$  angle. The average radius from all SIP measurements is 0.015199 inch and is considered to be accurate to within 10 microinches, corresponding to a computed viscosity within 0.5 micropoise.

Cross section or out-of-roundness profiles were taken with an Engis Equipment Company "Talyrond" Machine manufactured by Taylor, Taylor, and Hobson (Leicester, England). A special gaging stylus of approximately the same dimensions as the SIP stylus was used in the Talyrond instrument. The capillary tubes were held on the Talyrond in the same fixture utilized for SIP internal diameter measurements. The reference mark identified the Talyrond charts with the SIP measurements. The accuracy of the Talyrond is  $3 \times 10^{-6}$  inch, according to standards certified by the Atomic Energy Commission Primary Standards Laboratory (ALO), Albuquerque, New Mexico. This instrument charts deviation of the bore from a perfect circle on a greatly expanded scale. Three typical Talyrond charts are shown in figures 5, 6, and 7 and show, respectively, circular, trilobular, and irregular

---

Figure 5.-Cross section profile of a circular capillary bore.







TABLE 1. - Internal diameter measurements

<u>Sample number</u>	<u>Internal diameter, inch</u>			<u>Average radius, inch</u>
	0°	60°	120°	
1-1-A	0.03046	0.03045	0.03048	0.015232
1-1-B	.03057	.03049	.03041	.015245
2-1-A	.03039	.03035	.03044	.015197
2-1-B	.03051	.03041	.03031	.015205
3-1-A	.03039	.03040	.03041	.015200
3-1-B	.03045	.03046	.03043	<u>.015223</u>
				.015217
1-2-A	0.03041	0.03043	0.03048	0.015220
1-2-B	.03030	.03044	.03046	.015200
2-2-A	.03046	.03050	.03048	.015240
2-2-B	.03050	.03045	.03056	.015252
3-2-A	.03048	.03051	.03054	.015255
3-2-B	.03055	.03051	.03046	<u>.015253</u>
				.015237
1-3-A	0.03033	0.03035	0.03044	0.015187
1-3-B	.03058	.03052	.03046	.015260
2-3-A	.03047	.03043	.03054	.015240
2-3-B	.03044	.03049	.03042	.015225
3-3-A	.03043	.03039	.03030	.015187
3-3-B	.03043	.03031	.03035	<u>.015182</u>
				.015214
1-4-A	0.03031	0.03029	0.03030	0.015150
1-4-B	.03039	.03035	.03038	.015187
2-4-A	.03045	.03039	.03038	.015203
2-4-B	.03041	.03037	.03038	.015193
3-4-A	.03032	.03040	.03031	.015172
3-4-B	.03041	.03045	.03043	<u>.015215</u>
				.015187
1-5-A	0.03031	0.03036	0.03032	0.015165
1-5-B	.03040	.03039	.03038	.015195
2-5-A	.03045	.03039	.03041	.015208
2-5-B	.03038	.03041	.03036	.015192
3-5-A	.03045	.03046	.03039	.015217
3-5-B	.03043	.03035	.03038	<u>.015193</u>
				.015195







TABLE 1. - Internal diameter measurements - Continued

<u>Sample number</u>	<u>Internal diameter, inch</u>			<u>Average radius, inch</u>
	0°	60°	120°	
1-6-A	0.03036	0.03041	0.03043	0.015200
1-6-B	.03031	.03032	.03034	.015162
2-6-A	.03042	.03040	.03045	.015212
2-6-B	.03045	.03043	.03043	.015218
3-6-A	.03043	.03041	.03040	.015207
3-6-B	.03037	.03034	.03036	<u>.015178</u>
				.015196
1-7-A	0.03036	0.03033	0.03031	0.015167
1-7-B	.03041	.03032	.03036	.015182
2-7-A	.03042	.03036	.03039	.015195
2-7-B	.03038	.03037	.03041	.015193
3-7-A	.03042	.03046	.03037	.015208
3-7-B	.03040	.03043	.03042	<u>.015208</u>
				.015192
1-8-A	0.03038	0.03042	0.03042	0.015203
1-8-B	.03043	.03037	.03038	.015197
2-8-A	.03038	.03039	.30336	.015188
2-8-B	.03045	.03047	.03046	.015230
3-8-A	.03046	.03048	.03045	.015232
3-8-B	.03047	.03044	.03041	<u>.015220</u>
				.015212
1-9-A	0.03050	0.03041	0.03038	0.015215
1-9-B	.03039	.03036	.03042	.015195
2-9-A	.03047	.03041	.03045	.015222
2-9-B	.03043	.03046	.03037	.015210
3-9-A	.03044	.03037	.03035	.015193
3-9-B	.03040	.03045	.03044	<u>.015215</u>
				.015208
1-10-A	0.03046	0.03043	0.03040	0.015215
1-10-B	.03045	.03040	.03042	.015212
2-10-A	.03037	.03038	.03035	.015183
2-10-B	.03043	.03044	.03042	.015215
3-10-A	.03040	.03037	.03041	.015197
3-10-B	.03044	.03040	.03041	<u>.015208</u>
				.015205







TABLE 1. - Internal diameter measurements - Continued

Sample number	Internal diameter, inch			Average radius, inch
	0°	60°	120°	
1-11-A	0.03040	0.03036	0.03038	0.015190
1-11-B	.03039	.03041	.03037	.015195
2-11-A	.03039	.03034	.03036	.015182
2-11-B	.03038	.03041	.03037	.015193
3-11-A	.03040	.03041	.03038	.015198
3-11-B	.03041	.03039	.03041	<u>.015202</u>
				.015193
1-12-A	0.03036	0.03036	0.03035	0.015178
1-12-B	.03034	.03038	.03037	.015182
2-12-A	.03036	.03034	.03033	.015172
2-12-B	.03026	.03022	.03020	.015113
3-12-A	.03038	.03035	.03033	.015177
3-12-B	.03035	.03033	.03032	<u>.015167</u>
				.015165
1-13-A	0.03031	0.03034	0.03032	0.015162
1-13-B	.03035	.03040	.03035	.015183
2-13-A	.03038	.03034	.03040	.015187
2-13-B	.03040	.03043	.03042	.015208
3-13-A	.03036	.03042	.03037	.015192
3-13-B	.03042	.03040	.03042	<u>.015207</u>
				.015190
1-14-A	0.03038	0.03041	0.03039	0.015197
1-14-B	.03039	.03043	.03042	.015207
2-14-A	.03044	.03043	.03045	.015220
2-14-B	.03045	.03043	.03046	.015223
3-14-A	.03045	.03044	.03042	.015218
3-14-B	.03044	.03046	.03043	<u>.015222</u>
				.015214
1-15-A	0.03045	0.03048	0.03046	0.015232
1-15-B	.03041	.03044	.03047	.015220
2-15-A	.03042	.03042	.03045	.015215
2-15-B	.03040	.03040	.03041	.015202
3-15-A	.03040	.03044	.03044	.015213
3-15-B	.03045	.03045	.03042	<u>.015220</u>
				.015217







TABLE 1. - Internal diameter measurements - Continued

<u>Sample number</u>	<u>Internal diameter, inch</u>			<u>Average radius, inch</u>
	0°	60°	120°	
1-16-A	0.03041	0.03044	0.03045	0.015217
1-16-B	.03045	.03042	.03040	.015212
2-16-A	.03046	.03047	.03045	.015230
2-16-B	.03046	.03043	.03043	.015220
3-16-A	.03043	.03041	.03042	.015210
3-16-B	.03040	.03037	.03040	<u>.015195</u>
				.015214
1-17-A	0.03040	0.03039	0.03042	0.015202
1-17-B	.03043	.03042	.03040	.015208
2-17-A	.03045	.03044	.03046	.015225
2-17-B	.03041	.03039	.03040	.015200
3-17-A	.03034	.03038	.03033	.015175
3-17-B	.03032	.03035	.03035	<u>.015170</u>
				.015197
1-18-A	0.03037	0.03034	0.03033	0.015173
1-18-B	.03039	.03037	.03037	.015188
2-18-A	.03033	.03037	.03038	.015180
2-18-B	.03037	.03035	.03024	.015160
3-18-A	.03033	.03030	.03028	.015152
3-18-B	.03034	.03031	.03031	<u>.015160</u>
				.015169
1-19-A	0.03041	0.03036	0.03038	0.015192
1-19-B	.03033	.03024	.03026	.015138
2-19-A	.03034	.03032	.03023	.015148
2-19-B	.03027	.03030	.03034	.015152
3-19-A	.03030	.03029	.03034	.015155
3-19-B	.03031	.03032	.03032	<u>.015158</u>
				.015157



TABLE 1 - (continued) Internal diameter measurements - Continued

Sample Number	Internal Diameter			Average Internal Diameter
	Top	Bottom	Side	
1-18-A	0.0304	0.0304	0.0304	0.0304
1-18-B	0.0304	0.0304	0.0304	
2-18-A	0.0304	0.0304	0.0304	
2-18-B	0.0304	0.0304	0.0304	
3-18-A	0.0304	0.0304	0.0304	
3-18-B	0.0304	0.0304	0.0304	
0.0304				
1-17-A	0.0303	0.0303	0.0303	0.0303
2-17-B	0.0303	0.0303	0.0303	
2-17-A	0.0303	0.0303	0.0303	
2-17-B	0.0303	0.0303	0.0303	
3-17-A	0.0303	0.0303	0.0303	
3-17-B	0.0303	0.0303	0.0303	
0.0303				
1-18-A	0.0303	0.0303	0.0303	0.0303
1-18-B	0.0303	0.0303	0.0303	
2-18-A	0.0303	0.0303	0.0303	
2-18-B	0.0303	0.0303	0.0303	
3-18-A	0.0303	0.0303	0.0303	
3-18-B	0.0303	0.0303	0.0303	
0.0303				
1-19-A	0.0303	0.0303	0.0303	0.0303
1-19-B	0.0303	0.0303	0.0303	
2-19-A	0.0303	0.0303	0.0303	
2-19-B	0.0303	0.0303	0.0303	
3-19-A	0.0303	0.0303	0.0303	
3-19-B	0.0303	0.0303	0.0303	
0.0303				



DIMENSIONAL

<u>Sample number</u>	<u>Internal diameter, inch</u>		
	<u>0°</u>	<u>60°</u>	<u>120°</u>
<u>1-1-B</u>	<u>0.03057</u>	<u>0.03049</u>	<u>0.03041</u>

Talyrond

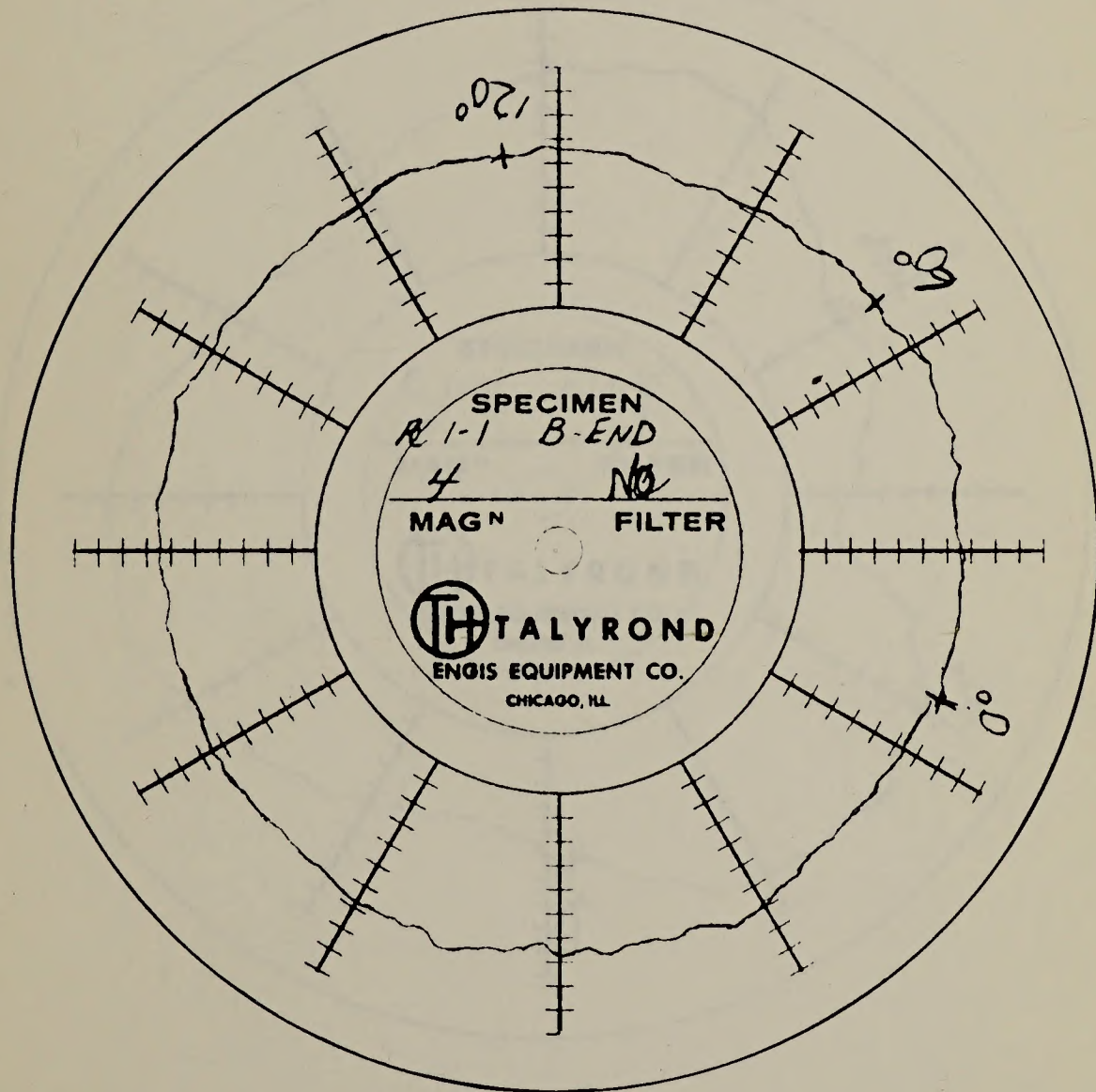


FIGURE 5.— Cross Section Profile of a Circular Capillary Bore







DIMENSIONAL

<u>Sample number</u>	<u>Internal diameter, inch</u>		
	<u>0°</u>	<u>60°</u>	<u>120°</u>
<u>1-15-A</u>	<u>0.03045</u>	<u>0.03048</u>	<u>0.03046</u>

Talyrond

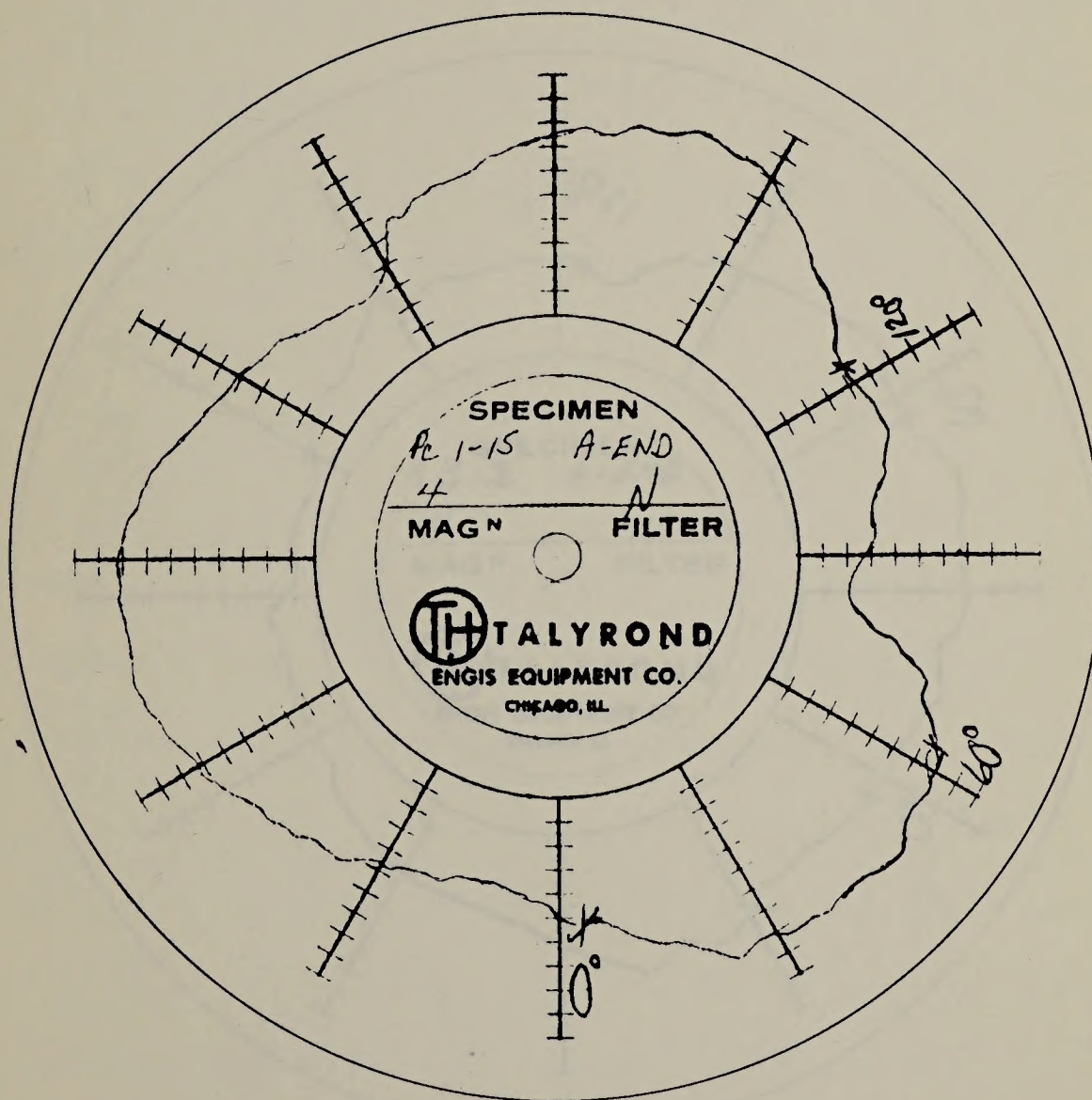


FIGURE 6.—Cross Section Profile of a Trilobular Capillary Bore



Sample number

1-15-A

0°

0.03045

50°

0.03048

150°

0.03048

lateral diameter, inch

lens

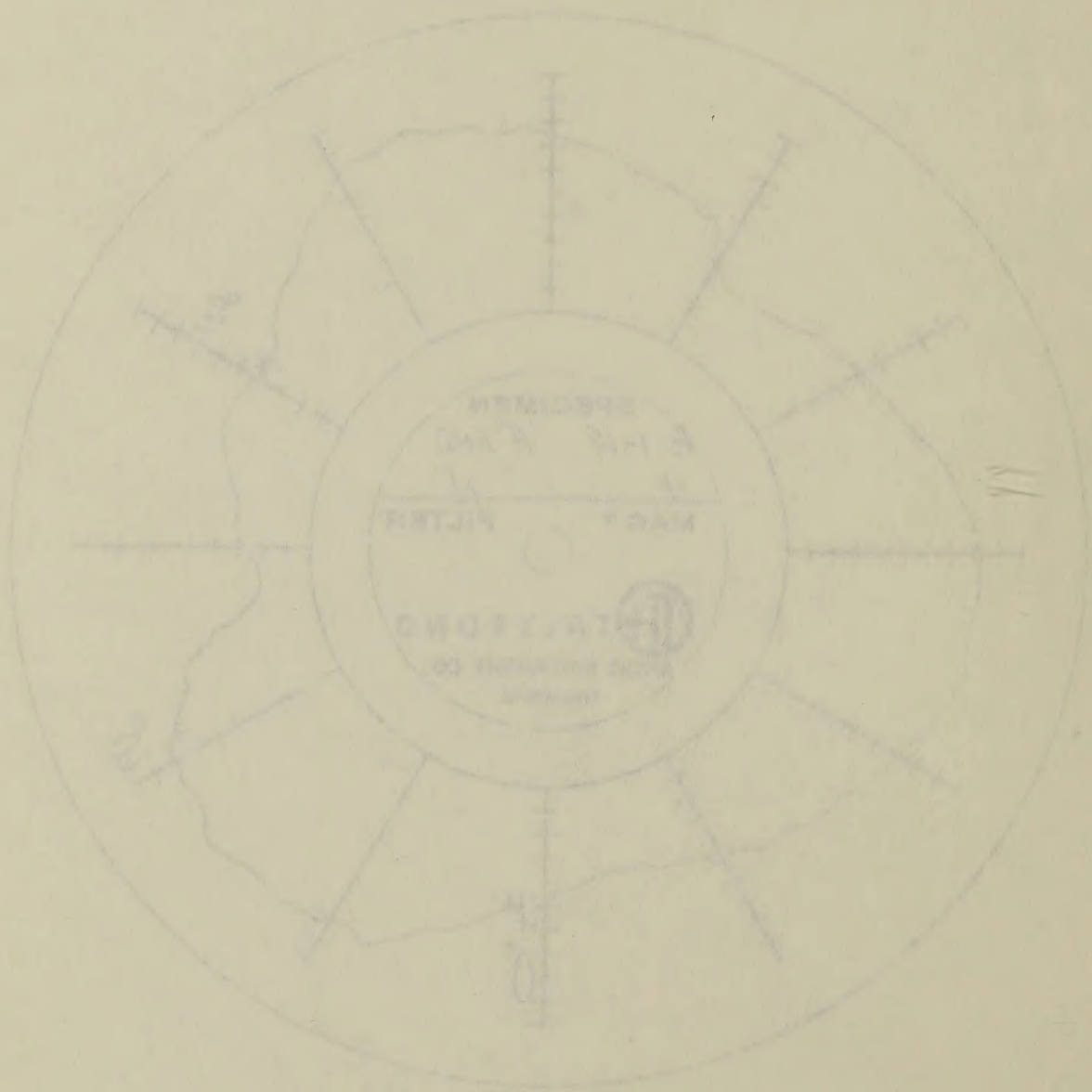


FIGURE 6.—Cross Section Profile of a Trilobular Capillary Bore



DIMENSIONAL

<u>Sample number</u>	<u>Internal diameter, inch</u>		
	<u>0°</u>	<u>60°</u>	<u>120°</u>
<u>3-2-A</u>	<u>0.03048</u>	<u>0.03051</u>	<u>0.03054</u>

Talyrond

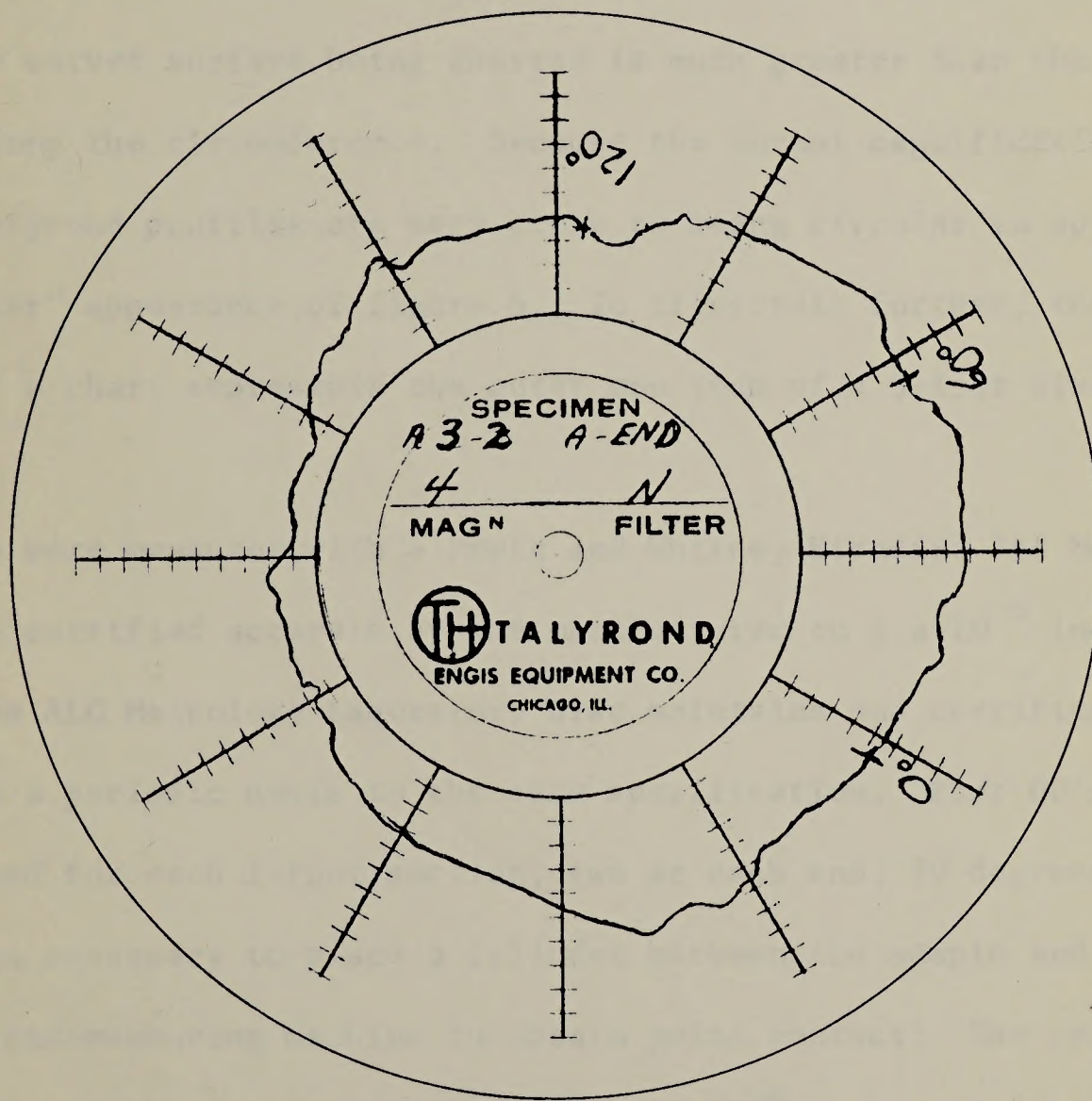


FIGURE 7. - Cross Section Profile of an Irregular Capillary Bore







Figure 6.-Cross section profile of a trilobular capillary bore.

Figure 7.-Cross section profile of an irregular capillary bore.

---

profiles. It is not necessary that the work be accurately centered in order to show true deviations from roundness.

Each Talyrond chart division represents  $50 \times 10^{-6}$  inch, reproducible to approximately the width of the trace. The magnification normal to the curved surface being charted is much greater than the magnification along the circumference. Because the normal magnification is 2,000, the Talyrond profiles are very close to being circular in spite of the "trilobular" appearance of figure 6. To illustrate further, the 1-inch scale of a chart represents the outer one inch of a 5-foot diameter circle.

The OD's were measured with a Pratt and Whitney Standard End Measuring Machine certified accurate by the manufacturer to  $5 \times 10^{-6}$  inch per inch. The ALO Metrology Laboratory also maintains and certifies the instrument on a periodic basis to the same specification. Four OD's were determined for each 1-foot section, two at each end, 90 degrees apart. It was necessary to place a cylinder between the sample and the anvil of the end-measuring machine to obtain point contact. The certified dimension of the cylinder, accurate to  $5 \times 10^{-6}$  inch, was subtracted from each reading to obtain the OD values listed in table 2. The apparent accuracy of the OD's is  $10 \times 10^{-6}$  inch. The average OD computed from all measurements is 0.122020 inch.







TABLE 2. - External diameter measurements

<u>Sample number</u>	<u>Outside diameter, inch</u>				<u>Average</u>
1	0.12214	0.12214	0.12203	0.12203	0.122085
2	.12210	.12202	.12212	.12208	.122080
3	.12209	.12207	.12212	.12211	.122098
4	.12210	.12206	.12215	.12207	.122095
5	.12197	.12205	.12206	.12206	.122035
6	.12211	.12197	.12214	.12199	.122052
7	.12192	.12180	.12205	.12195	.121930
8	.12202	.12199	.12212	.12200	.122032
9	.12202	.12200	.12203	.12199	.122010
10	.12200	.12195	.12204	.12201	.122000
11	.12211	.12196	.12203	.12196	.122015
12	.12204	.12205	.12210	.12205	.122060
13	.12206	.12197	.12203	.12201	.122018
14	.12204	.12195	.12213	.12209	.122052
15	.12202	.12199	.12195	.12194	.121975
16	.12189	.12199	.12213	.12202	.122008
17	.12180	.12186	.12204	.12195	.121912
18	.12200	.12187	.12212	.12191	.121975
19	.12195	.12201	.12193	.12190	.121948







The 1-foot sections were weighed on a 2-kilogram capacity analytical balance to 0.1 milligram. The National Bureau of Standards method of transposition (8)<sup>4/</sup> was used with certified stainless steel standard

---

<sup>4/</sup>Underlined numbers in parentheses refer to items in the list of references at the end of this report.

---

weights. Results of the weighings are given in table 3. The average apparent mass versus brass is 1.420717 grams per inch with an average deviation of  $\pm 0.00041$ .

The lengths of the 1-foot sections are given in table 3. With a section placed in the fixture (figure 1), a "best size" measuring wire was inserted in each end of the tube to establish the true centerline. The SIP optical system was used to measure the chord length from the center of the bore at one end to the center of the bore at the other end. The arc length (length of bore) was computed from:

$$L = \frac{\pi (10.00000 + a) \theta}{180}, \quad (2)$$

where "a" is one-half the average OD of the bore, and  $\theta$  is the angle of the sector in degrees.

Longitudinal internal surface finish measurements were taken with a Taylor, Taylor, and Hobson "Talysurf" Surface Finish Measuring Machine, which charted both surface finish and waviness relative to a 1-microinch optically-flat reference master. The readout capability of this instrument is  $5 \times 10^{-7}$  inch with interpolation to  $1 \times 10^{-7}$  inch







TABLE 3. - Length and mass measurements

Sample number	Length (chord), in	Length (arc), in	Apparent mass vs brass, g	True mass, g
1	11.22542	11.90849	16.93405	16.93417
2	.18213	.85637	16.85823	16.85835
3	.28229	.97709	17.02168	17.02180
4	.21809	.89966	16.91229	16.91241
5	.24830	.93607	16.95357	16.95369
6	.24382	.93067	16.94858	16.94870
7	.21662	.89790	16.89985	16.89997
8	.23920	.92510	16.94461	16.94473
9	.19920	.87692	16.87065	16.87077
10	.22077	.90289	16.91059	16.91071
11	.21817	.89976	16.90626	16.90638
12	.19385	.87047	16.86611	16.86623
13	.22249	.90496	16.90857	16.90869
14	.20648	.88568	16.88125	16.88137
15	.23230	.91679	16.91755	16.91767
16	.21202	.89235	16.89588	16.89600
17	.19275	.86916	16.86279	16.86291
18	.21400	.89474	16.88976	16.88988
19	.17942	.85312	16.83715	16.83727







along 1/4-inch lengths of exposed surface. The accuracy of surface finish measurements is considered one microinch, including procedural and calibration errors. Arithmetically averaged internal surface roughnesses were five, eight, six, eight, eight, and six microinches. Any minor projection or burr in the capillary wall which is less than 10 microinches will not measurably affect the laminar flow profile.

#### CONFIRMATION OF MEAN RADIUS THROUGH TALYROND CHARTS

The Talyrond measures out-of-roundness, not actual diameter. The determination of an average "cross sectional" radius from a Talyrond chart depends on relating the chart scale to the diameters measured directly with the SIP. This was accomplished using the SIP reference 0° mark at each end of the 4-inch sections. When the sections were run on the Talyrond, each chart was marked at 0°, 60°, and 120°. In figure 5, "bottom of scale" is the inner circle from which the chart scales radiate at 30-degree intervals. Each division of a chart scale is 0.1 inch, and represents  $50 \times 10^{-6}$  inch actual travel by the Talyrond stylus. The chart diameter at "bottom of scale" is two inches. The "equivalent distance at bottom of scale" was determined at each known diameter (0°, 60°, 120°) by measuring the distance across the chart trace, subtracting the chart diameter at "bottom of scale" (two inches), and dividing by 0.1 inch per division to get the number of chart divisions. The accuracy of measuring the distance across the chart was 0.01 inch corresponding to 0.000005 inch in determining "equivalent distance at bottom of scale" and is well within the accuracy of the SIP. The







chart divisions were converted to actual inches by multiplying by  $50 \times 10^{-6}$  inch per division. This number was subtracted from the corresponding measured SIP diameter to give "equivalent diameter at bottom of scale." The "equivalent radius at bottom of scale" for each Talyrond chart is the average of the three "equivalent diameters," divided by two.

The area enclosed by the line traced on the chart was measured with a planimeter calibrated in square inches. The radius of a true circle having the same area was computed; the chart radius at bottom of scale (one inch) was subtracted from the computed radius, and the remainder was converted to chart divisions (0.1 inch = one division). The chart division value was converted to actual inches (times  $50 \times 10^{-6}$ ) and added to the "equivalent radius at bottom of scale." This procedure gave an average radius for each of the 114 cross sections as shown in table 4. The average of all cross sections is 0.015201 inch, which compares very favorably with the 0.015199 inch SIP average and provides confirmation of the SIP diameters. A sample calculation follows for Talyrond chart sample 1-1-B (figure 5).

Equivalent distance at bottom of scale:

$$\begin{aligned} 0^\circ: 3-25/64 \text{ in} - 2 \text{ in} &= 1.391 \text{ in} = 13.91 \text{ div} = 0.000695 \text{ in;} \\ 60^\circ: 3-5/16 \text{ in} - 2 \text{ in} &= 1.312 \text{ in} = 13.12 \text{ div} = 0.000656 \text{ in;} \\ 120^\circ: 3-5/16 \text{ in} - 2 \text{ in} &= 1.312 \text{ in} = 13.12 \text{ div} = 0.000656 \text{ in.} \end{aligned}$$

Equivalent diameter at bottom of scale:

$$\begin{aligned} 0^\circ: 0.03057(\text{SIP}) - 0.000695 &= 0.029875 \text{ in;} \\ 60^\circ: 0.03049(\text{SIP}) - 0.000656 &= 0.029834 \text{ in;} \end{aligned}$$







TABLE 4. - Radii computed by integrating the Talyrond charts

<u>Sample number</u>	<u>Talyrond radius, inch</u>	<u>Last 3 digits of average SIP</u>	<u>Sample number</u>	<u>Talyrond radius, inch</u>	<u>Last 3 digits of average SIP</u>
1-1-A	0.015234	232	1-2-A	0.015220	220
1-1-B	.015237	245	1-2-B	.015194	200
2-1-A	.015193	197	2-2-A	.015244	240
2-1-B	.015200	205	2-2-B	.015242	252
3-1-A	.015195	200	3-2-A	.015274	255
3-1-B	<u>.015218</u>	<u>223</u>	3-2-B	<u>.015272</u>	<u>253</u>
Average	.015213	217	Average	.015241	237
1-3-A	0.015180	187	1-4-A	0.015140	150
1-3-B	.015259	260	1-4-B	.015206	187
2-3-A	.015246	240	2-4-A	.015200	203
2-3-B	.015215	225	2-4-B	.015196	193
3-3-A	.015172	187	3-4-A	.015175	172
3-3-B	<u>.015182</u>	<u>182</u>	3-4-B	<u>.015204</u>	<u>215</u>
	.015209	214		.015187	187
1-5-A	0.015156	165	1-6-A	0.015200	200
1-5-B	.015202	195	1-6-B	.015176	162
2-5-A	.015216	208	2-6-A	.015210	212
2-5-B	.015187	192	2-6-B	.015224	218
3-5-A	.015214	217	3-6-A	.015222	207
3-5-B	<u>.015202</u>	<u>193</u>	3-6-B	<u>.015186</u>	<u>178</u>
	.015197	195		.015203	196
1-7-A	0.015193	167	1-8-A	0.015214	203
1-7-B	.015196	182	1-8-B	.015195	197
2-7-A	.015200	195	2-8-A	.015202	188
2-7-B	.015203	193	2-8-B	.015239	230
3-7-A	.015214	208	3-8-A	.015238	232
3-7-B	<u>.015217</u>	<u>208</u>	3-8-B	<u>.015235</u>	<u>220</u>
	.015204	192		.015220	212
1-9-A	0.015226	215	1-10-A	0.015212	215
1-9-B	.015203	195	1-10-B	.015208	212
2-9-A	.015230	222	2-10-A	.015194	183
2-9-B	.015221	210	2-10-B	.015207	215
3-9-A	.015187	193	3-10-A	.015207	197
3-9-B	<u>.015226</u>	<u>215</u>	3-10-B	<u>.015210</u>	<u>208</u>
	.015215	208		.015206	205







TABLE 4. - Radii computed by integrating the Talyrond charts  
Continued

Sample number	Talyrond radius, inch	Last 3 digits of average SIP	Sample number	Talyrond radius, inch	Last 3 digits of average SIP
1-11-A	0.015201	190	1-12-A	0.015171	178
1-11-B	.015202	195	1-12-B	.015199	182
2-11-A	.015183	182	2-12-A	.015177	172
2-11-B	.015200	193	2-12-B	.015112	113
3-11-A	.015218	198	3-12-A	.015181	177
3-11-B	<u>.015195</u>	<u>202</u>	3-12-B	<u>.015176</u>	<u>167</u>
	.015200	193		.015170	165
1-13-A	0.015168	162	1-14-A	0.015199	197
1-13-B	.015176	183	1-14-B	.015201	207
2-13-A	.015174	187	2-14-A	.015239	220
2-13-B	.015221	208	2-14-B	.015235	223
3-13-A	.015195	192	3-14-A	.015213	218
3-13-B	<u>.015215</u>	<u>207</u>	3-14-B	<u>.015239</u>	<u>222</u>
	.015192	190		.015221	214
1-15-A	0.015233	232	1-16-A	0.015222	217
1-15-B	.015223	220	1-16-B	.015214	212
2-15-A	.015229	215	2-16-A	.015223	230
2-15-B	.015218	202	2-16-B	.015225	220
3-15-A	.015210	213	3-16-A	.015190	210
3-15-B	<u>.015232</u>	<u>220</u>	3-16-B	<u>.015185</u>	<u>195</u>
	.015224	217		.015210	214
1-17-A	0.015205	202	1-18-A	0.015175	173
1-17-B	.015216	208	1-18-B	.015190	188
2-17-A	.015226	225	2-18-A	.015173	180
2-17-B	.015199	200	2-18-B	.015172	160
3-17-A	.015176	175	3-18-A	.015154	152
3-17-B	<u>.015173</u>	<u>170</u>	3-18-B	<u>.015171</u>	<u>160</u>
	.015199	197		.015172	169
1-19-A	0.015189	192			
1-19-B	.015144	138			
2-19-A	.015124	148			
2-19-B	.015143	152			
3-19-A	.015154	155			
3-19-B	<u>.015167</u>	<u>158</u>			
	.015154	157			







$$120^\circ:0.03041(\text{SIP}) - 0.000656 = \underline{0.029744} \text{ in};$$

$$\text{Average} = 0.029818 \text{ in.}$$

$$\text{Equivalent radius at bottom of scale} = 0.014909 \text{ in.}$$

$$\text{Area measured by planimeter} = 8.62 \text{ in}^2.$$

$$\text{Radius of circle with same area} = (8.62/\pi)^{1/2} = 1.656 \text{ in};$$

$$1.656 - 1.000 = 0.656 \text{ in} = 6.56 \text{ chart div};$$

$$(6.56 \text{ chart div})(50 \times 10^{-6} \text{ in/div}) = 0.000328.$$

$$\text{Average radius of cross section (1-1-B)} = 0.014909 + 0.000328;$$

$$= 0.015237 \text{ in.}$$

$$\text{Average radius of three (1-1-B) SIP measurements} = 0.015245.$$

#### CORRECTION FOR NON-UNIFORMITY OF CAPILLARY BORE

Capillary tube viscosimeters can be considered as an infinite number of uniform, right circular cylinders arranged in series. This concept leads to correcting the hypothetical mean radius,  $R_m$ , in equation (1) to approximate more closely the real case and has been discussed by Barr (1, p. 61), Flynn (3, p. 25), Giddings (4, p. D-8), Lemaire (7, p. 21), and Swindells and coworkers (10, p. 17). This report designates the correction as

$$\delta = \frac{\sum_{i=1}^n \left(\frac{R_m}{R_i}\right)^4}{n} = \frac{\sum_{i=1}^n \left(\frac{L_i}{R_i^4}\right)}{\left(\frac{L_T}{R_m^4}\right)}, \quad (3)$$

where  $L_i$  is a constant or  $L_i = L_1 = L_2 = L_3 = \dots = L_n$ . Ideally,  $n$  is infinite. In the practical case, however,  $n$  can be some finite number







of samples whereby the evaluation of  $\delta$  and its insertion into equation (1) may or may not be of significance in computing viscosity, depending on the magnitude of the non-uniformity of the capillary bore. Utilizing the 114 individual SIP radii leads to a value for  $\delta$  of 1.000030;  $\delta$  equals 1.000035 using the individual Talyrond radii. In either case, the error in computing viscosity is less than 0.01 micropoise when the viscosity is 200 micropoises.

In computing  $\delta$  from the average radii tabulated in table 1, the following procedure was used. For sample 1-1-A, the front end of the first 4-inch sample, the average radius of 0.015232 inch was assumed to apply to the first two inches; the average radius for the back end (1-1-B) of this same 4-inch sample, 0.015245 inch, was assumed to apply to the other two inches of this sample. In other words, each averaged radius in table 1 represents a uniform bore of 2-inch length,  $L_i$ .

Figure 8 shows the deviation of the 19-foot capillary bore from the

---

Figure 8.-Deviation of the capillary bore from the average radius.

---

average SIP radius,  $R_m$ , in millionths of an inch. The plotted values are the 1-foot averages shown in the last column of table 1; the maximum deviation is about 40 millionths of an inch.

Figure 9 is a frequency distribution graph of the 342 SIP diameter

---

Figure 9.-Distribution of SIP diameter measurements.

---







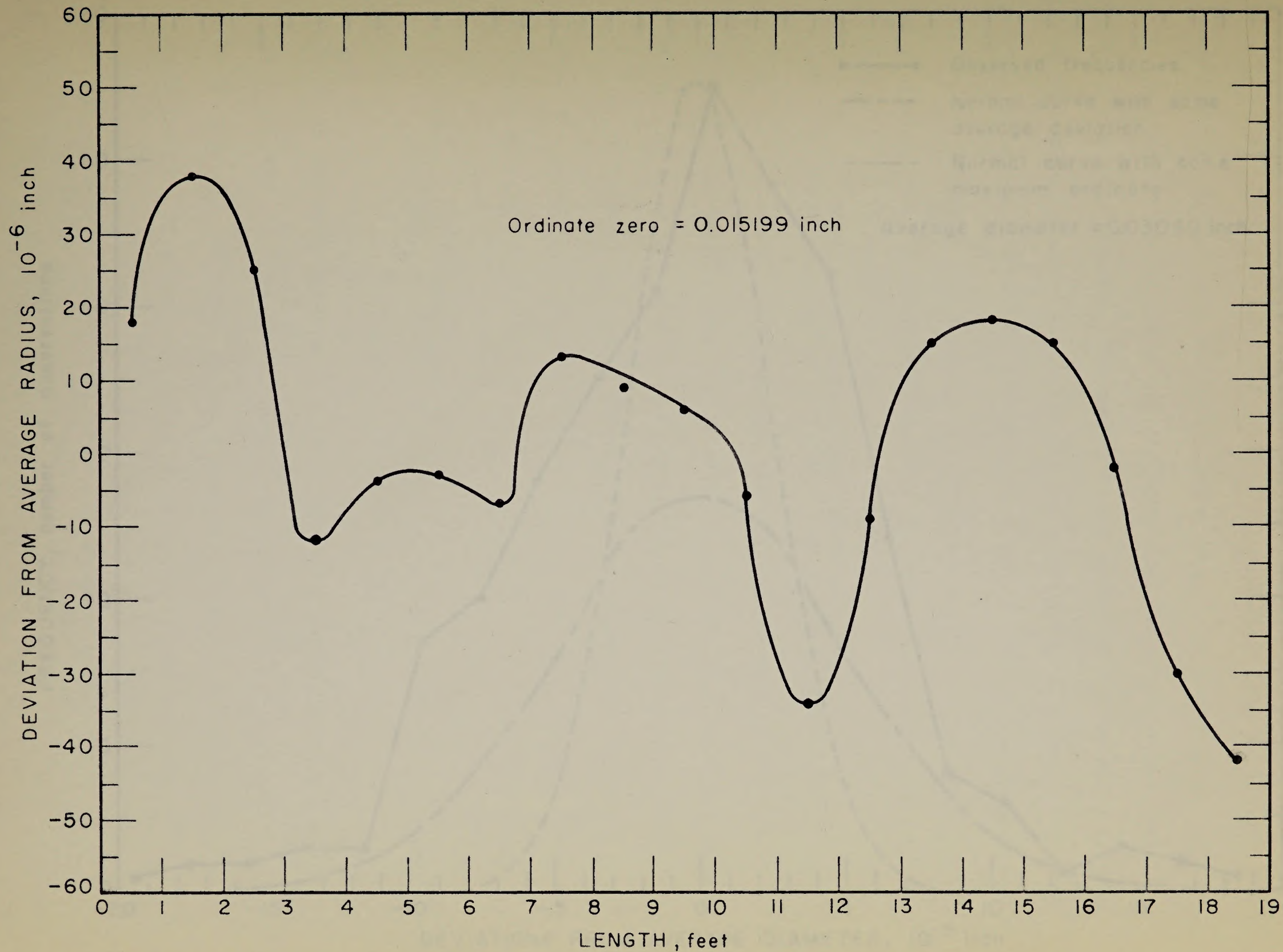


FIGURE 8.-Deviation of the Capillary Bore from the Average Radius







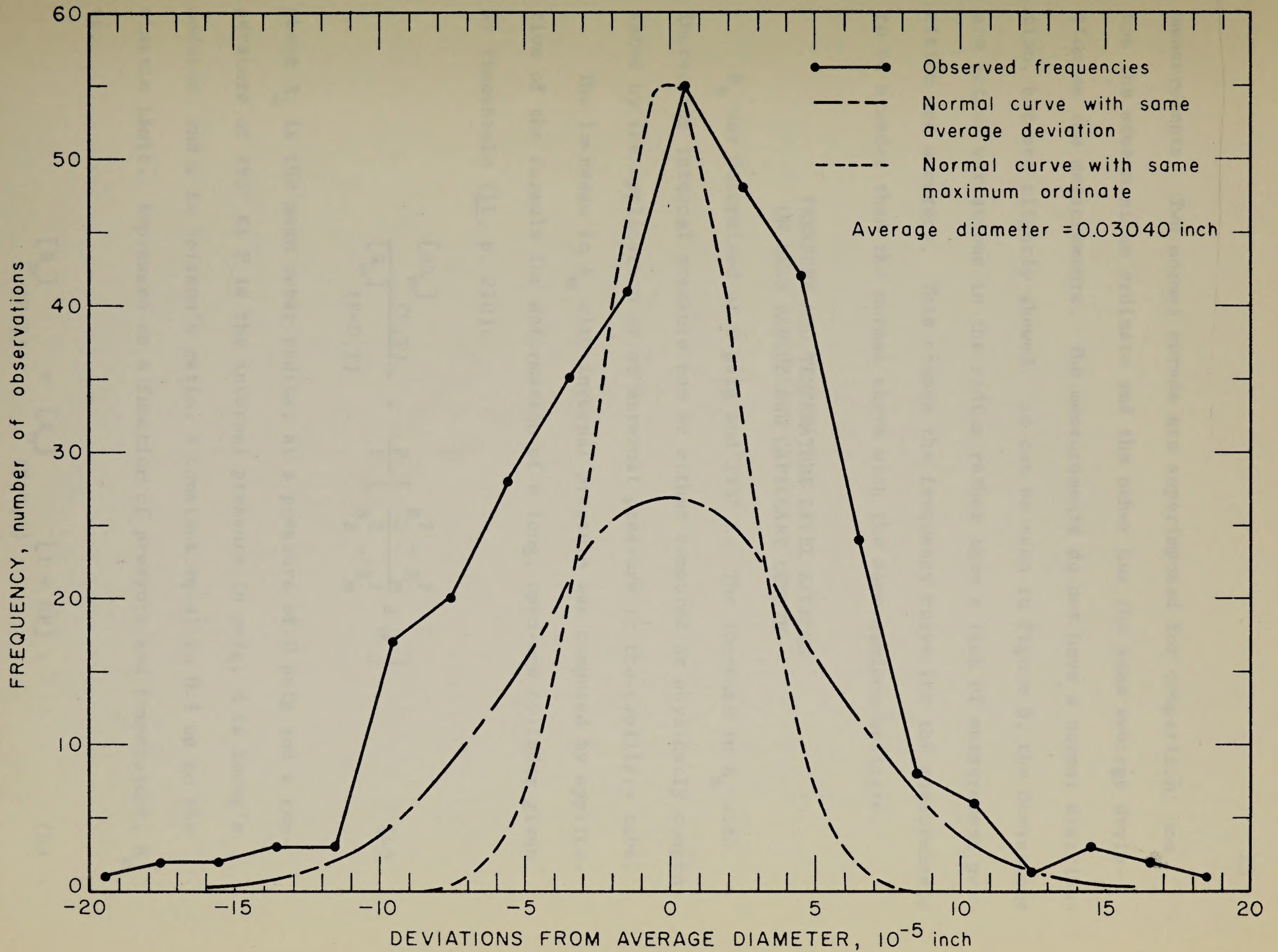


FIGURE 9.-Distribution of SIP Diameter Measurements







measurements. Two normal curves are superimposed for comparison; one has the same maximum ordinate and the other has the same average deviation as the measurements. The measurements do not have a normal distribution, but are slightly skewed. As can be seen in figure 8, the deviations are actual variations in the radius rather than a lack of measurement precision and accuracy. This causes the frequency curve for the measurements to be broader than the normal curve with the same maximum ordinate.

#### PRESSURE AND TEMPERATURE LEVEL EFFECTS ON MEAN RADIUS AND CAPILLARY LENGTH

$R_m$  was determined at 0 psig and 293° K. The increase in  $R_m$  with increasing internal pressure can be either computed or physically compensated by the application of an external pressure to the capillary tube.

The increase in  $R_m$  with internal pressure was computed by application of the formula for deformation of a long, open-end cylinder given by Timoshenko (11, p. 210):

$$\frac{[\Delta R_m]_{(P,T)}}{[R_m]_{(P=0,T)}} = \frac{P}{E} \left[ \frac{R_2^2 + R_m^2}{R_2^2 - R_m^2} + \mu \right], \quad (4)$$

where  $R_2$  is the mean outer radius, at a pressure of 0 psig and a temperature of 293° K;  $P$  is the internal pressure in psig;  $E$  is Young's modulus; and  $\mu$  is Poisson's ratio, a constant equal to 0.3 up to the elastic limit. Expressed as a function of pressure and temperature,  $R_m$  is:

$$[R_m]_{(P,T)} = [R_m]_{(P=0,T)} [1 + \beta P], \quad (5)$$



measurements. Two normal curves are superimposed for comparison; one has the same maximum ordinate and the other has the same average deviation as the measurements. The measurements do not have a normal distribution, but are slightly skewed. As can be seen in figure 8, the deviations are normal variations in the radius rather than a lack of measurement precision and accuracy. This causes the frequency curve for the measurements to be broader than the normal curve with the same maximum ordinate.

INTERNAL PRESSURE AND THE CAPILLARY RADIUS

The increase in  $R_0$  with internal pressure was measured by applying increasing internal pressure and by either expanding or physically compressing the capillary tube. The increase in  $R_0$  with internal pressure was measured by application of the formula for deformation of a long, cylindrical vessel given by Timoshenko (11, p. 210):

$$\frac{\Delta R_0}{R_0} = \frac{p}{E} \left[ \frac{1}{2} \left( \frac{R_0^2}{r^2} + \frac{1}{2} \right) + \frac{1}{2} \left( \frac{R_0^2}{r^2} - \frac{1}{2} \right) \right] \quad (8)$$

where  $R_0$  is the mean outer radius, at a pressure of  $p$  psi, and a constant of  $10^3$ ;  $E$  is the internal pressure in psi;  $r$  is Young's modulus; and  $\nu$  is Poisson's ratio, a constant equal to 0.3 up to the elastic limit. Expressed as a function of pressure and temperature,  $R_0$

$$R_0 = R_0(p, T) = R_0(0, T) + \Delta R_0(p, T) \quad (9)$$



where  $\beta$ , the pressure expansion coefficient, is:

$$\beta = \frac{1}{E} \left[ \frac{R_2^2 + R_m^2}{R_2^2 - R_m^2} + \mu \right]. \quad (6)$$

Also,

$$[R_m]_{(P=0, T)} = [R_m]_{(P=0, 293^\circ K)} [1 + \alpha \Delta T], \quad (7)$$

where  $\alpha$  is the thermal expansion coefficient.

The thermal expansion coefficient,  $\alpha$ , of 347 stainless steel is given by Corruccini and Gniewek (2, p. 12) and Schwartzberg and coworkers (9, p. B.7.t); Young's modulus as a function of temperature is given by the latter (9, p. B.7.ij). From these references it was determined that:

$$\alpha = f(T) = C_1 + C_2 T + C_3 T^2 \quad (8)$$

and

$$\beta = f(T) = (C_4 + C_5 \Delta T), \quad (9)$$

where  $C_1$ ,  $C_2$ ,  $C_3$ ,  $C_4$ , and  $C_5$  are constants,  $T$  is degrees Kelvin, and

$\Delta T = T - 293$ ; the values of the constants are:  $C_1 = 1.07418 \times 10^{-5}$ ,

$C_2 = 2.97565 \times 10^{-8}$ ,  $C_3 = -4.230 \times 10^{-11}$ ,  $C_4 = 5.502 \times 10^{-8}$ , and  $C_5 = 1.97 \times 10^{-11}$ .

Therefore,

$$[R_m]_{(P, T)} = [R_m]_{(P=0, 293^\circ K)} [1 + \alpha \Delta T][1 + \beta P]. \quad (10)$$







The capillary length as a function of temperature is:

$$L_T = f(T) = [L_T]_{(293^\circ\text{K})} [1 + (C_1 + C_2T + C_3T^2) \Delta T], \quad (11)$$

where  $C_1$ ,  $C_2$ ,  $C_3$ ,  $T$ , and  $\Delta T$  are the same as previously defined.

Incorporating the temperature and pressure corrections into equation (1) gives

$$\eta = \left[ \frac{\pi \Delta P_e [R_m^4]_{(P=0, 293^\circ\text{K})}}{8 Q_m L_{(293^\circ\text{K})}} \right] \left[ 1 + (C_1 + C_2T + C_3T^2) \Delta T \right]^3 \left[ 1 + (C_4 + C_5 \Delta T) P \right]^4, \quad (12)$$

as  $\delta$  was shown to be negligible.

Over the pressure range 28 to 1,000 psia, the calculated change in  $R_m$  is less than 10 microinches. Higher internal pressures will significantly affect viscosity calculations. Both  $L_T$  and  $R_m$  change with temperature by approximately 0.001 percent per degree Kelvin. Because the viscosimeter will be operated over wide ranges of temperature and pressure, both corrections are retained in the final working equation for viscosity, equation (12).

#### AVERAGE RADIUS AND DENSITY EVALUATION BY DIFFERENT METHODS

Superior Tube Company suggested a value of 0.2833 lb/in<sup>3</sup> for the density of the 347 stainless steel tubing, based on mole percent weight-







ing from composition analysis. Specific gravity determinations, using distilled water, by the Pantex facility gave  $0.2862 \text{ lb/in}^3$  for a randomly-selected, 1-foot section. An average density of  $0.2856 \text{ lb/in}^3$  was computed from the average SIP  $R_m$  and the volumetric method (page 7). The latter density value was taken to be the most accurate.

Values for  $R_m$  were computed by the volumetric method using the Superior Tube Company and Pantex densities. Using a gas expansion technique<sup>5</sup> which is independent of density,  $R_m$  values were determined

---

<sup>5</sup>Further information regarding the gas expansion technique developed at the Helium Research Center is available upon request from the Research Director, Helium Research Center, Bureau of Mines, Amarillo, Texas.

---

for the 32- and 208-foot long capillary tubes as well as an 85-foot long section. These data are summarized in table 5.

#### ENTRANCE, KINETIC ENERGY, GAS SLIPPAGE, AND GAS COMPRESSIBILITY EFFECTS

The entrance and kinetic energy effects are discussed together; the effects of gas slippage and gas compressibility are examined similarly. These are applied to the 32-foot (971.704 cm) long capillary in the form of a coil 20 inches in diameter using nitrogen at  $300^\circ \text{ K}$  and pressure levels of 28 and 1,000 psia. It is assumed, a priori, that entrance, kinetic energy, and gas slippage effects for straight tube capillaries apply to the coil.







TABLE 5. -Average radius and density evaluation by different methods

Density, lb/in <sup>3</sup>	Source	Method	R <sub>m</sub> , in <sup>1/</sup>	L <sub>T</sub> , ft
0.2833	Superior Tube Company	Volumetric	0.014281	19
.2862	Pantex Plant	-----do-----	.015492	19
-----	Helium Research Center	Gas expansion	.015334	32
-----	-----do-----	-----do-----	.015399	85
-----	-----do-----	-----do-----	.015130	208
<u>2/</u> .2856	-----do-----	SIP	.015199	19

1/ Average, not including SIP, equals 0.015127 in;  
average, gas expansion, equals 0.015287 in;  
average, all, equals 0.015305 in.

2/ Computed from SIP and volumetric measurements.







Entrance and Kinetic Energy Effects

Couette suggested correcting Poiseuille's equation for external resistance for the case of flow streamlines entering a thick-walled capillary from a larger conduit, past a square-cut end; further, Brillouin showed that this could be expressed as a hypothetical addition to the length,  $L_T$ . The expression for this extra length is  $nR_m$  where  $n$  is a constant between 0.8 and 0.9. The work of Couette and Brillouin is detailed by Barr (1, p. 20). Using a value of 0.9 for  $n$  and 0.0152017 inch (0.0386 cm) for  $R_m$  yields at 300° K and 1,000 psia:

$$L_T + nR_m = 971.742 \text{ cm} . \quad (13)$$

A calculated viscosity of 200.06 micropoises changes to 200.05 by correcting for the entrance effect. This change is negligible.

The kinetic energy correction, as shown by Barr (1, p. 15) and Swindells and coworkers (10, p. 2), results from acceleration of the streamlines after entering the constricted capillary and is included in the measured pressure drop,  $\Delta P_{me}$ . If the assumptions are made that steady-state laminar volumetric flow exists at the entrance and that the same kinetic energy is retained throughout the capillary (that is,  $Q_m$  is constant), then:

$$\Delta P_{me} = \Delta P_e + \Delta P_{Ke} , \quad (14)$$

where  $\Delta P_e$  is the pressure drop used to overcome viscous resistance and  $\Delta P_{Ke}$  is the pressure drop due to kinetic energy. By way of Barr (1, p. 17), it can be shown that:







$$\Delta P_e = \Delta P_{me} - \frac{m\rho Q_m^2}{\pi^2 R_m^4}, \quad (15)$$

where  $m$  is a characteristic physical constant nearly equal to unity and  $\rho$  is the density of the flowing fluid. The kinetic energy correction for short capillaries at high volumetric flow rates is significant.

At 1,000 psia and 300° K, the density of nitrogen was interpolated to be 0.07428 g/cm<sup>3</sup> from Flynn (3, p. 123). Average experimental values for  $Q_m$  and  $\Delta P_{me}$  were 0.02222 cm<sup>3</sup>/sec and 0.0678 psi, respectively. For these conditions  $R_m$  equals 0.0152017 inch or 0.038612 cm. Substituting into equation (15) gives, for the last term, a value of 1.67 dynes/cm<sup>2</sup> or about  $2.4 \times 10^{-5}$  psi which is negligible compared to  $\Delta P_{me}$ . A viscosity of 200 micropoises would change by 0.05 micropoise by making the correction.

#### Gas Slippage and Gas Compressibility Effects

By kinetic theory considerations it can be deduced that, in the immediate vicinity of the capillary wall, a layer of gas thinner than the mean free path,  $\lambda$ , of the molecules has a finite velocity (slip) in the direction of flow. It can be shown by way of Klinkenberg (6, p. 4) that the modified Poiseuille equation, corrected for gas slippage, is

$$\eta = \left[ \frac{\pi R_m^4 \Delta P_e}{8L_T Q_m} \left( 1 + \frac{4c\lambda}{R_m} \right) \right]_{(T,P)}, \quad (16)$$







where  $c$  is a numerical constant nearly equal to unity. According to Guevara and Wageman (5, p. 19), this constant has been calculated to be 1.147. A reasonable estimate of the effect of slippage, the term in parentheses, needs to be made at the lowest pressure level, 28 psia, because slippage is more significant at low pressures (and temperatures).

From Flynn (3, pp. 123, 127), extrapolated density and viscosity values for nitrogen at 28 psia and 298° K were  $2.33 \times 10^{-3}$  g/cm<sup>3</sup> and 178 micropoises, respectively. The mean free path was computed to be  $488 \times 10^{-8}$  cm from simple kinetic theory considerations;  $\lambda$  equals  $3\eta/\rho\bar{c}$ , where  $\bar{c}$  is the average molecular speed. The value of  $4\lambda/R_m$  at 298° K, assumed to apply at 300° K, was evaluated to be  $506 \times 10^{-6}$  cm. The value of the slippage term is 1.000506, corresponding to a viscosity correction of 0.1 micropoise.

The differential equation for isothermal steady-state laminar flow of compressible fluids, neglecting slippage, is:

$$Q_m \int_0^{L_T} dL = - \frac{\pi R_m^4}{8\eta} \int_{P_1}^{P_2} \left[ \left( \frac{Z_m}{Z} \right) \left( \frac{P}{P_m} \right) \right] dP, \quad (17)$$

where  $Z_m$  is the compressibility factor for the fluid at the mean system pressure,  $P_m = (P_1 + P_2)/2$ , and  $Q_m$  is the volumetric flow rate at  $P_m$ .

For nitrogen, the change in  $Z$  from the entrance of the capillary ( $P_1$ ) to the exit ( $P_2$ ) is approximately  $1 \times 10^{-5}$  at 300° K. The pressure drop across the 32-foot long capillary, at 28 and 1,000 psia, was less







than one psi. The ratio  $Z_m/Z$ , then, is so close to unity that it can be removed from the integral and the compressible gas treated as incompressible as long as this condition obtains.

#### SUMMARY

Special methods have been developed for measuring physical dimensions of small diameter tubing, and for evaluating the parameters associated with Poiseuille-type viscometry which are inherently dependent on those dimensions. As far as the authors are aware, this study represents the first time that a long section of stainless steel capillary tubing has been comprehensively examined by metrological methods for use in an absolute gas viscosimeter. As the capillary mean radius is considered accurate to 10 millionths of an inch, viscosities can be determined to one micropoise or better. An accurate appraisal of the non-uniformity of the capillary bore, or variations of radius along the length, is made. Although the individual radii are slightly skewed from a normal distribution, the deviations are actual variations in radii rather than a lack of measurement precision. The internal surface finish of the tubing will not measurably affect the viscosity determinations.

The effects of pressure and temperature on the mean radius and overall length are incorporated into a final working equation for viscosity. Corrections for bore non-uniformity, entrance effects, kinetic energy effects, and gas slippage, all implied to be negligible for the tubing used at low volumetric flow rates, can be included in the final working equation for greater accuracy. The capillary internal diameter measure-







ment and its accuracy, however, are the most significant physical parameters in capillary tube viscometry. Because of the very small pressure drops across the system, the gas is treated as an incompressible fluid.

2. Corradi, Robert J., and John J. Gilweck. Thermal Expansion of Technical Solids at Low Temperatures. NBS Monograph 79, Nov 1961, 24 pp.
3. Flynn, George Patrick. The Viscosity of Nitrogen and Argon as a Function of Density and Temperature. Ph. D. thesis, Brown University, June 1967, 143 pp.
4. Siddons, John G. The Viscosity of Light Hydrocarbon Mixtures at High Pressures: The Methane-Propane System. Ph. D. thesis, Rice University, May 1963, p. D-4.
5. Conway, F. A., and V. L. Wagner. Measurements of Helium and Hydrogen Viscosities to 1.49° K. Los Alamos Scientific Laboratory, Los Alamos, New Mexico, 1965, 43 pp.
6. Klinkenberg, L. A. The Permeability of Porous Media to Liquids and Gases. Eleventh Mid-Year Meeting of the American Petroleum Institute, Tulsa, Oklahoma, May 27, 1961, 12 pp.
7. Lewis, Norman Arthur. The Viscosity of Helium and Neon as a Function of Density and Temperature. Ph. D. thesis, Brown University, June 1967, 141 pp.
8. NBS. Design and Test of Standards of Mass. NBS Circ. No. 3, December 27, 1918, pp. 37-38. Paper on NBS Handbook 77, Precision Measurement and Calibration, v. 3, Optics, Metrology, and Radiation, February 1, 1961, pp. 425-436.







## REFERENCES

1. Barr, Guy. A Monograph of Viscometry. Oxford University Press, London, 1931, 318 pp.
2. Corruccini, Robert J., and John J. Gniewek. Thermal Expansion of Technical Solids at Low Temperatures. NBS Monograph 29, May 1961, 24 pp.
3. Flynn, George Patrick. The Viscosity of Nitrogen and Argon as a Function of Density and Temperature. Ph. D. thesis, Brown University, June 1962, 145 pp.
4. Giddings, John G. The Viscosity of Light Hydrocarbon Mixtures at High Pressures: The Methane-Propane System. Ph. D. thesis, Rice University, May 1963, p. D-8.
5. Guevara, F. A., and W. E. Wageman. Measurement of Helium and Hydrogen Viscosities to 2,340° K. Los Alamos Scientific Laboratory, Los Alamos, New Mexico, 1965, 43 pp.
6. Klinkenberg, L. J. The Permeability of Porous Media to Liquids and Gases. Eleventh Mid-Year Meeting of the American Petroleum Institute, Tulsa, Oklahoma, May 22, 1941, 12 pp.
7. Lemaire, Normand Arthur. The Viscosity of Helium and Neon as a Function of Density and Temperature. Ph. D. thesis, Brown University, June 1962, 141 pp.
8. NBS. Design and Test of Standards of Mass. NBS Circ. No. 3, December 23, 1918, pp. 37-38. Paper in NBS Handbook 77, Precision Measurement and Calibration, v. 3, Optics, Metrology, and Radiation, February 1, 1961, pp. 655-656.







## REFERENCES (Con.)

9. Schwartzberg, F. R., S. H. Osgood, R. D. Keys, and T. F. Kiefer. Cryogenic Materials Data Handbook. U. S. Department of Commerce, July 1965, pp. B.7.ij and B.7.t.
10. Swindells, J. F., J. R. Coe, Jr., and T. B. Godfrey. Absolute Viscosity of Water at 20° C. NBS J. Res., v. 48, No. 1, January 1952, 31 pp.
11. Timoshenko, S. Strength of Materials, pt. 2, Advanced Theory and Problems. D. Van Nostrand Co., Inc., Princeton, N. J., 1956, 3rd ed., 572 pp.



















